

The genetic organization of *Desulfovibrio desulphuricans* ATCC 27774 bacterioferritin and rubredoxin-2 genes: involvement of rubredoxin in iron metabolism

Patrícia N. da Costa,¹ Célia V. Romão,¹ Jean LeGall,² António V. Xavier,¹ Eurico Melo,¹ Miguel Teixeira¹ and Lígia M. Saraiva^{1*}

¹*Instituto de Tecnologia Química e Biológica, Universidade Nova de Lisboa, R. da Quinta Grande 6, 2780-156 Oeiras, Portugal.*

²*Department of Biochemistry, University of Georgia, Athens, GA 30602, USA.*

Summary

The anaerobic bacterium *Desulfovibrio desulphuricans* ATCC 27774 contains a unique bacterioferritin, isolated with a stable di-iron centre and having iron-coproporphyrin III as its haem cofactor, as well as a type 2 rubredoxin with an unusual spacing of four amino acid residues between the first two binding cysteines. The genes encoding for these two proteins were cloned and sequenced. The deduced amino acid sequence of the bacterioferritin shows that it is among the most divergent members of this protein family. Most interestingly, the *bacterioferritin* and *rubredoxin-2* genes form a dicistronic operon, which reflects the direct interaction between the two proteins. Indeed, bacterioferritin and rubredoxin-2 form a complex *in vitro*, as shown by the significant increase in the anisotropy and decay times of the fluorescence of rubredoxin-2 tryptophan(s) when mixed with bacterioferritin. In addition, rubredoxin-2 donates electrons to bacterioferritin. This is the first identification of an electron donor to a bacterioferritin and shows the involvement of rubredoxin-2 in iron metabolism. Furthermore, analysis of the genomic data for anaerobes suggests that rubredoxins play a general role in iron metabolism and oxygen detoxification in these prokaryotes.

Introduction

Ferritins are a widespread class of proteins involved in iron

storage (Theil, 1987; Harrison and Arosio, 1996). In some organisms, a subfamily of these proteins containing a haem cofactor is present, which was named bacterioferritins as they were first found in bacteria (Stiefel and Watt, 1979; Andrews, 1998). Although the role of ferritins in aerobes in iron storage and protection from iron-mediated oxidative stress is relatively well established (Harrison and Arosio, 1996; Waldo and Theil, 1996), their function in anaerobes remains less understood (Rocha *et al.*, 1992; Ratnayake *et al.*, 2000; Romão *et al.*, 2000a).

The bacterioferritin (Bfr) from the sulphate-reducing bacterium *Desulfovibrio desulphuricans* ATCC 27774 (*Dd27k*) is, so far, the only bacterioferritin isolated from an anaerobic organism (Romão *et al.* 2000a). In contrast to other bacterioferritins, *Dd27k* Bfr contains a new type of biological haem cofactor, the iron-coproporphyrin III (Romão *et al.*, 2000b), a haem quite distinct from the haem B usually found in bacterioferritins (Bulen *et al.*, 1973; Yariv *et al.*, 1981; Frolow *et al.*, 1994; Andrews, 1998). Also, *Dd27k* Bfr is the only known example of a ferritin isolated with a stable di-iron centre (Romão *et al.*, 2000a; Coelho *et al.*, 2001), the site for the initial oxidation of ferrous iron in the process of iron storage.

Rubredoxins are small, monomeric and mononuclear iron proteins found in many prokaryotes (Sieker *et al.*, 1994), as well as in some eukaryotes (Tabata *et al.*, 2000; Wastl *et al.*, 2000; Zauner *et al.*, 2000). All the studied sulphate-reducing bacteria belonging to the genus *Desulfovibrio* contain at least one rubredoxin (type 1 Rd, named Rd-1). In *Desulfovibrio vulgaris* Hildenborough (*DvH*) and *Dd27k*, besides Rd-1, another type of rubredoxin (type 2 Rd, named Rd-2) was detected, which mainly differs from Rd-1 in the spacing between the cysteine ligands: the first two cysteines-binding motif –Cys-xx-Cys– is substituted by –Cys-xxxx-Cys– in Rd-2 (Lumppio *et al.*, 1997; LeGall *et al.*, 1998).

The genomic organization of the genes coding for rubredoxins is quite diverse, reflecting their various physiological roles as one-electron carriers, which parallels the wide range of reduction potentials of rubredoxins or Rd sites in complex proteins. Its reduction potentials vary from –150 mV (Swartz *et al.*, 1996; Eidsness *et al.*, 1999; Yoon *et al.*, 1999; Gomes *et al.*,

Accepted 27 April, 2001. *For correspondence. E-mail lst@itqb.unl.pt; Tel. (+351) 2144 69834; Fax (+351) 2144 28766.

2000) to $\approx +230$ mV in rubrerythrin (LeGall *et al.*, 1988). In the sulphate-reducing bacterium *Desulfovibrio gigas*, rubredoxin-1 plays a role in oxygen reduction, being the direct electron donor to a terminal oxygen reductase (Chen *et al.*, 1993; Gomes *et al.*, 1997); in other anaerobes, rubredoxins can function as electron acceptors for diverse enzymes, such as pyruvate or carbon monoxide dehydrogenases (Ragsdale *et al.*, 1983; Yoon *et al.*, 1999).

Because of the unique characteristics of *Dd27k* bacterioferritin and Rd-2, the determination of their complete amino acid sequences as well as their genetic organization was performed. In this paper, it is shown that the *bfr* and *rd-2* genes are located in tandem forming a single transcriptional unit, reflecting the function of Rd-2 in the iron metabolism of *Dd27k*, as electron donor to the bacterioferritin. Using fluorescence spectroscopy, it is also shown that Rd-2 and Bfr form a complex *in vitro*. Analysis of the full sequenced genomes of several anaerobic prokaryotes suggests that rubredoxins may play a role in prokaryotic iron metabolism, closely associated with oxygen detoxification processes.

Results and discussion

Nucleotide and complete amino acid sequence of *Dd27k* Rd-2

The 2.5 kb *EcoRI*–*SphI* insert of plasmid pUBfRd contains a 189 nucleotide (nt) open reading frame (ORF), which is preceded by a ribosome binding site (RBS) (GGAGG) 5 bp upstream of the start codon (Fig. 1). The deduced amino acid sequence of 62 residues predicts a molecular mass of 7.2 kDa, and the identity between the first 39 residues and the published N-terminal sequence (LeGall *et al.*, 1998) confirms the cloning of *Dd27k* Rd-2 (Fig. 2).

The amino acid sequence of *Dd27k* Rd-2 shows a high degree of similarity to other rubredoxins, isolated from either *Desulfovibrio* species or more distant organisms (Fig. 2). The highest similarity is found with *DvH* Rd-2 (60% identity and 68% similarity); *Dd27k* and *DvH* Rd-2 are, so far, the only two examples of rubredoxins presenting the unusual spacing –Cys-xxxx-Cys– at the first cysteine-binding motif. Taking into account the spacing between these cysteine residues, another type of rubredoxin, which we propose to name type 3 rubredoxin (Rd-3) for consistency, is present in *Methanococcus jannaschii*, with

a motif –Cys-x-Cys– (Bult *et al.*, 1996). An extension of this type of classification would include as a fourth type the small rubredoxin-type protein, desulphoredoxin (Dx), so far isolated only from *D. gigas*, in which the second cluster of cysteines has no amino acids in between (–CysCys–) (Bruschi *et al.*, 1979). However, the overall amino acid identity (or similarity) between Dx and Dx-like domains in desulphoferrodoxins (Ascenso *et al.*, 2000) and rubredoxins is extremely small, suggesting that they may be only distantly related. All rubredoxins and many rubredoxin domains in more complex proteins exhibit considerable amino acid conservation: several amino acid residues are strictly or almost strictly conserved (Fig. 2), namely the aromatic amino acids that form a hydrophobic core underneath the iron centre (Sieker *et al.*, 1994). This conservation does not appear to be related to the specific physiological partner, rather suggesting a structural role (Kummerle *et al.*, 1997; Moulis, 1999). Also, in contrast to recent proposals (Swartz *et al.*, 1996) for the division of rubredoxins according to the type of residue after the second cysteine motif –CysPro–x–CysGly–z, with z being an alanine or a valine, it is clear that quite a large variability exists at this site.

Nucleotide and complete amino acid sequence of *Dd27k* Bfr

Upstream of the start codon of the *rd-2* gene, a 540 nt ORF (with RBS sequence AGGAG located 8 bp upstream of the start codon) is observed (Fig. 1). This ORF encodes a potential 19.9 kDa protein with a deduced amino acid sequence of 179 residues. As the first 74 residues of the gene-derived sequence are identical to the published N-terminal sequence of *Dd27k* bacterioferritin (Romão *et al.*, 2000a), and the predicted molecular mass (20 kDa) agrees with the reported value, we conclude that this DNA sequence encodes the Bfr protein from *Dd27k*.

The complete amino acid sequence shows that *Dd27k* Bfr is one of the more divergent bacterioferritins sequenced so far. In fact, the multiple amino acid sequence alignment of bacterioferritins (Fig. 3) shows that a lower degree of conservation is observed between the amino acid sequence of *Dd27k* Bfr and the other Bfrs (22–28%) when compared with the range of values usually observed (36–70%). A BLAST search against the incomplete genome of *D. vulgaris* Hildenborough revealed the presence of a similar bacterioferritin (66% identity). In

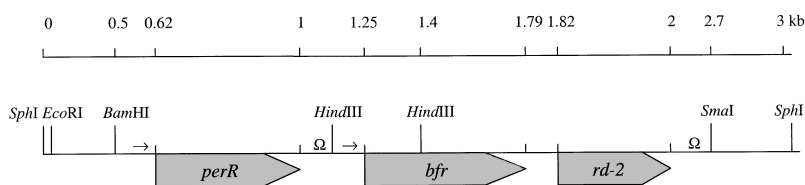


Fig. 1. Genetic map of the 3 kb *EcoRI*–*SphI* fragment harbouring *perR*, *bfr* and *rd-2* genes of *Dd27k*. The restriction sites for *SphI*, *EcoRI*, *BamHI*, *HindIII* and *SmaI* are indicated. Putative promoters are indicated by (→) and probable terminators by (Ω). The direction of transcription is also shown.

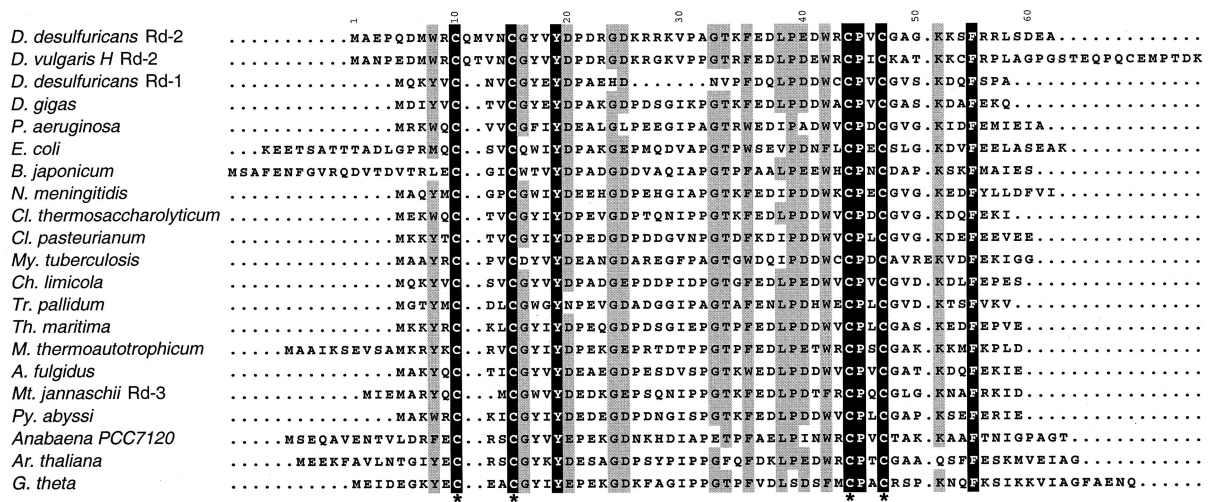


Fig. 2. Amino acid sequence alignment of *Dd27k* Rd-2 with other rubredoxins from representative prokaryotes and from eukaryotes (% identity, NCBI-GI). Type 2 rubredoxins: *DvH* (60%, 1769572). Type 1 rubredoxins: *Dd27k* (31%, 134112); *D. gigas* (42%, 134113); *Pseudomonas* (*P.*) *aeruginosa* (36%, 11352532); *E. coli* (28%, 882603); *Bradyrhizobium* (*B.*) *japonicum* (27%, 1351031); *Neisseria* (*N.*) *meningitidis* (36%, 11249911); *Clostridium* (*Cl.*) *thermosaccharolyticum* (42%, 134111); *Cl. pasteurianum* (36%, 231175); *Mycobacterium* (*My.*) *tuberculosis* (34%, 7430809); *Chlorobium* (*Ch.*) *limicola* (42%, 134107); *Treponema* (*Tr.*) *pallidum* (36%, 7430808); *Thermotoga* (*Th.*) *maritima* (39%, 4981182); *Methanobacterium* (*M.*) *thermoautotrophicum* (42%, 7430810); *Archaeoglobus* (*A.*) *fulgidus* (41%, 11498486); *Pyrococcus* (*Py.*) *abyssi* (44%, 7521668); *Anabaena PCC7120* (31%, 5139323); *Arabidopsis* (*Ar.*) *thaliana* (30%, 4585992); *Guillardia* (*G.*) *theta* (27%, 4583668). Type 3 rubredoxins: *Methanococcus* (*Mt.*) *jannaschii* (41%, 2117423). The sequences from *Anabaena PCC7120*, *Ar. thaliana* and *G. theta* are shown only in the region containing the rubredoxin fold (residues 1–67 for *Anabaena PCC7120*, residues 88–154 for *Ar. thaliana* and residues 57–122 for *G. theta*). The cysteines involved in iron co-ordination (stars) are shown below the alignment. Black boxes represent conserved residues, and grey boxes represent almost strictly conserved residues.

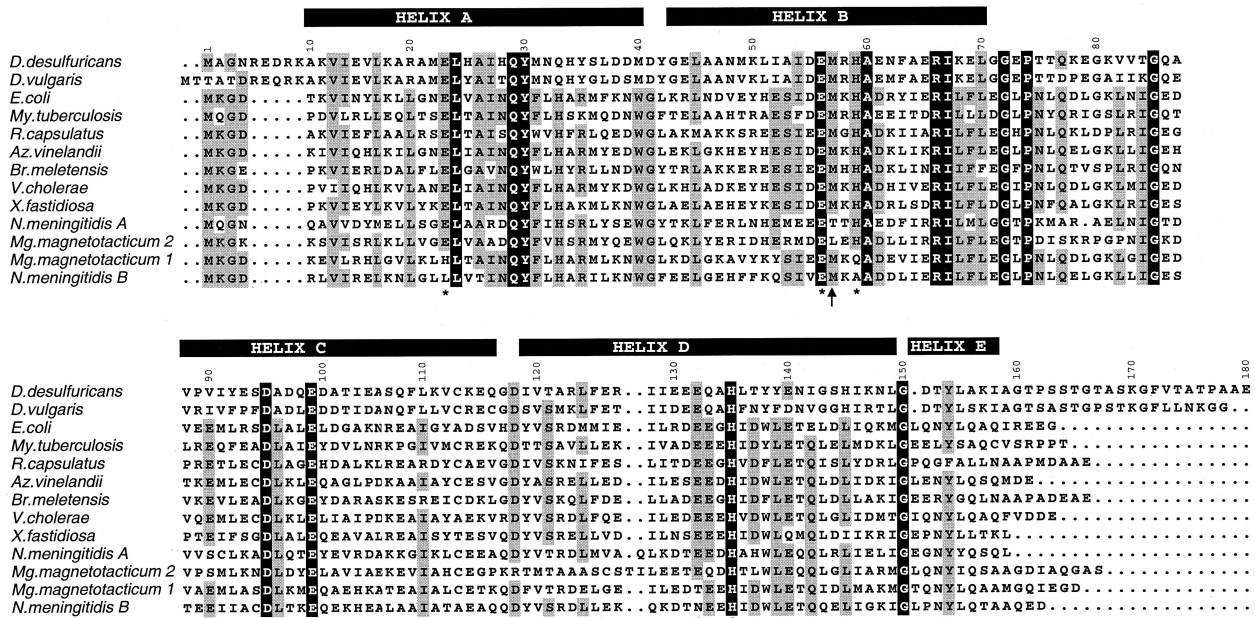


Fig. 3. Amino acid sequences of bacterioferritin from *Dd27k* and from other bacteria (% identity, NCBI-GI). *E. coli* (25%, 114932), *My. tuberculosis* (28%, 2225984), *Rhodobacter* (*R.*) *capsulatus* (28%, 2493294), *Azotobacter* (*Az.*) *vinelandii* (26%, 114931), *Brucella* (*Br.*) *melitensis* (26%, 1705456), *Vibrio* (*V.*) *cholerae* (27%, 9654782), *Xylella* (*X.*) *fastidiosa* (26%, 9105231), *Magnetospirillum* (*Mg.*) *magnetotacticum* 1 and 2 (24%, 2688837; 24%, 2688836), *N. meningitidis* A and B (22%, 7226444; 25%, 7226443), *DvH* genome (66%). The regions of *E. coli* bacterioferritin corresponding to the α -helices (A–E) are shown above the alignment, and the ligands to the di-iron centre (stars) and the haem methionine ligand (arrow) are shown below the alignment. Black boxes represent conserved residues, and grey boxes represent almost strictly conserved residues.

spite of the low amino acid similarity of Bfr from *Dd27k* (and *DvH*) to other bacterioferritins, some important residues are still strictly conserved (*Dd27k* Bfr numbered and location according to the tridimensional structure of *Escherichia coli* Bfr): (i) all the residues binding the di-iron centre, Glu-23, Glu-56, Glu-99, Glu-132, His-59 and His-135; (ii) the haem iron axial ligand, Met-57; (iii) Tyr-30, hydrogen bonded to Glu-99, proposed to be involved in the formation of a transient tyrosyl-radical species during the iron oxidation/storage reaction (Harrison and Arosio, 1996); (iv) Gln-29 and Asp-95, which are in ionic interaction; and (v) Arg-66, Ser/Thr-121 and Asp-118, probably involved in a network of hydrogen bonds.

Contrary to what is observed in all other bacterioferritins, instead of protoporphyrin IX (Frolow *et al.*, 1994; Andrews, 1998), *Dd27k* Bfr contains iron-coproporphyrin III as haem cofactor (Romão *et al.*, 2000b). The presence of the different haem side-chains may result in an increase in the number of residues in the vicinity of the haem that are in electrostatic or hydrogen bonding interaction with it. Hence, the low amino acid sequence identity may reflect, at least in part, the presence of the different cofactor. The preliminary X-ray crystallography data also show that the protein forms a 24-mer (Coelho *et al.*, 2001), and that each monomer has the same four-helix bundle fold characteristic of all (bacterio)ferritins.

Upstream of the gene encoding for *Dd27k* Bfr, an ORF of 408 nt with the RBS sequence (GGAGG) located 7 bp upstream of its start codon (Fig. 1), encodes a predicted protein of 136 residues (15 kDa) (data not shown). A BLASTX GenBank search for this protein revealed a significant degree of sequence identity with several peroxidase-like repressor proteins (PerR) (22–28%) (Bsat *et al.*, 1998) and, in particular, with the PerR-like protein from *DvH* (55% identity), which was initially classified as a ferric uptake regulator (Fur)-like protein (Lumppio *et al.*, 1997).

As the region upstream of the *bfr* gene in *Neisseria gonorrhoeae* contains a Fur binding sequence (Chen and Morse, 1999), these typical patterns were searched in the upstream region of *Dd27k bfr*, but they were not detected.

Organization and transcriptional analysis of the *Dd27k* perR–bfr–rd-2 gene cluster

The *perR*-like, *bfr* and *rd* genes are localized in tandem and transcribed in the same direction (Fig. 1). Although 255 nt separates the stop codon of the *perR*-like gene and the start codon of *bfr*, an intervening gap of only 28 nt separates the *bfr* and *rd-2* genes. Upstream of the start codon of the *perR*-like gene, putative –35 and –10 promoter regions were detected (data not shown), and 118 bp downstream of the stop codon in *perR* lies a GC-rich region of dyad symmetry, perhaps signalling a

transcription terminator. In the 255 nt region, 19 nt upstream of the start codon in the *bfr* gene, a putative transcriptional promoter sequence was also identified and, 35 bp downstream of the stop codon in *rd*, a hairpin loop-forming structure that may serve as a *rho*-independent transcription terminator is observed. Hence, the overall organization suggests that, in *Dd27k*, the PerR-like protein is encoded by a monocistronic gene, and the closely spaced *bfr* and *rd* genes form an operon (Fig. 1).

To confirm this genetic organization, Northern analyses of total RNA isolated from nitrate-grown *Dd27k* cells were performed (Fig. 4, lanes 1–3 and 5). The transcriptional experiments revealed the presence of a single transcript of 850 ± 30 bp, using either the *bfr*-RNA (Fig. 4, lanes 1–4) or the *rd*-RNA probes (Fig. 4, lane 5), which corresponds, within the experimental error, to the sum of the sizes of the *bfr* and *rd* genes. Furthermore, no difference in the size and intensity of the transcript was observed between the RNAs isolated from nitrate-grown cells collected in the initial, mid-log and late-exponential phases (Fig. 4). Northern analysis performed using RNA isolated from sulphate-grown *Dd27k* cells (Fig. 4, lane 4) proved that the *bfr* and *rd* genes form a dicistronic operon that is

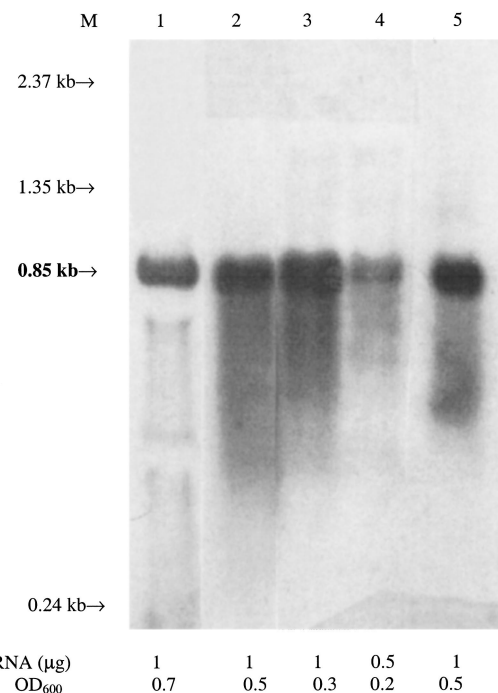


Fig. 4. Transcriptional analysis of the *Dd27k bfr*–*rd-2* operon. Northern blots of *Dd27k* total RNA probed with *bfr*-RNA (lanes 1–4) and *rd-2*-RNA (lane 5). Lanes (1–3 and 5) contain 1 µg of total RNA extracted from *Dd27k* cells grown anaerobically with nitrate and collected at the late (OD₆₀₀ = 0.7), mid-log (OD₆₀₀ = 0.5) and initial (OD₆₀₀ = 0.3) exponential phases. Lane 4 contains 0.5 µg of total RNA extracted from *Dd27k* cells grown anaerobically with sulphate and collected at the initial exponential phase (OD₆₀₀ = 0.2). M, molecular mass standards; the size determined for the *bfr*–*rd-2* mRNA is indicated in bold.

expressed under both sulphate or nitrate growth conditions.

In sulphate reducers, Rd-1s are encoded in dicistronic units together with genes for enzymes involved in oxygen detoxification (Fig. 5): rubredoxin:oxygen-oxidoreductase in *D. gigas* (Chen *et al.*, 1993; Gomes *et al.*, 1997; Frazão *et al.*, 2000) or desulphoferrodoxins (Brumlik and Voordouw, 1989; Pianzola *et al.*, 1996; Kitamura *et al.*, 1997; Liochev and Fridovich, 1997; Romão *et al.*, 1999). In *DvH*, *rd-2* is present in a gene cluster that includes rubrerythrin and a *perR*-like gene (Lumppio *et al.*, 1997; Bsat *et al.*, 1998). It was proposed that the three genes form an operon (Fig. 5), although a shorter transcript corresponding only to the sum of the *rubredoxin* and *rubrerythrin* gene sizes was also observed (Lumppio *et al.*, 1997). Despite these results, the physiological role of Rd-2 in *DvH* remains unknown. Our results clearly show that, in *Dd27k*, the *perR*-like gene does not belong to the *bfr*–*rd-2* operon (Figs 1 and 5). In *Dd27k*, the operon formed by *rd-2* and *bfr* suggests a function for Rd-2 in iron metabolism (see below). So far, the only other known similar genetic organization occurs in *Methanobacterium thermoautotrophicum*, in which rubredoxins are also encoded by genes close to that encoding for a ferritin (Smith *et al.*, 1997). Quite interestingly, this gene cluster also includes an A-type flavoprotein, a homologue of *D. gigas* rubredoxin:oxygen-oxidoreductase, as well as a superoxide dismutase and an alkyl hydroperoxide reductase (Fig. 5), suggesting a quite close association of the iron and oxygen responses in this archaeon. In other organisms, such as *E. coli* and *Azotobacter vinelandii*, (*bacterio*)*ferritin* genes are located immediately downstream of an ORF that encodes for a $[2\text{Fe}-2\text{S}]^{2+/1+}$ protein, named

bacterioferritin-associated ferredoxin (Bfd). In *E. coli*, Bfd was proposed to be a redox and/or regulator component of bacterioferritin, because it appears to form a complex with this protein (Garg *et al.*, 1996). Although no relevant amino acid similarity is observed between *Dd27k* Rd-2 and the various Bfds ($\approx 14\%$), a similar role may be performed by the two different proteins, as will be discussed below.

Interaction between *Dd27k* Rd-2 and Bfr

Recombinant *Dd27k* Rd-2 was isolated from a culture of BL21-Gold(DE3) carrying pT7Rd2, as described in *Experimental procedures*. SDS–PAGE of cell extracts and of the purified Rd-2 revealed a strong band of ≈ 8 kDa (Fig. 6) that agrees with the molecular mass predicted by the gene-derived amino acid sequence of *Dd27k* Rd-2. Upon purification, two rubredoxin-2 forms were obtained, either zinc or iron bound: ZnRd-2 and FeRd-2. The recombinant FeRd-2 showed no differences when compared with the wild-type *Dd27k* Rd-2 in the UV/visible and EPR spectra, confirming the presence of an intact metal centre. Both proteins contain a stoichiometric amount of one metal per molecule.

The genetic organization of *Dd27k* *bfr* and *rd-2* suggests a possible interaction between the two proteins. To prove this interaction, two different approaches were used: a fluorescence study, measuring the average lifetime and the steady-state anisotropy of the tryptophans (Trp) in Rd-2, in the absence and in the presence of Bfr; and a redox interaction, followed by visible spectroscopy, to check whether Bfr is reduced by Rd-2. The fluorescence assays were performed with ZnRd-2, which has a much more intense fluorescence emission when compared with the iron form.

The fluorescence emission of ZnRd-2, when excited at 300 nm, is an unstructured band with a maximum at 330 nm (Fig. 7, curve a). In Fig. 7, curve c represents the excitation spectrum of ZnRd-2 in the same conditions when the emission is collected at 350 nm. Both, excitation and emission are characteristic of tryptophan (Trp) and are attributed to the two tryptophan residues existing in the molecule (Fig. 2). Under the same excitation and emission conditions and in the concentrations used in this work, the fluorescence of Bfr is comparatively much lower than that of ZnRd-2 (Fig. 7, curves b and d). Namely, when excited at 300 nm, the emission at 350 nm is ≈ 13 times less intense than that of ZnRd-2 (Fig. 7, curves a and b). In the subsequent study of steady-state fluorescence anisotropy and fluorescence lifetimes, the samples were excited at 300 nm and 292 nm, respectively, and the emission was collected at 350 nm. In these conditions and for the purpose of the present work, the contribution of Bfr emission is negligible.

The fluorescence decay of ZnRd-2, excited at 292 nm, is

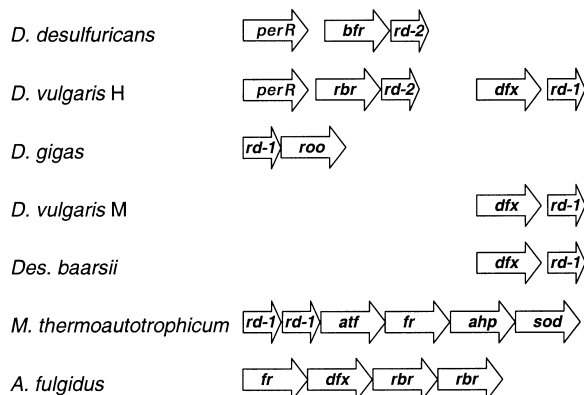


Fig. 5. Genomic organization of the genes encoding rubredoxin and ferritin proteins from the archaea *M. thermoautotrophicum* and *A. fulgidus*, and the bacteria *Dd27k*, *DvH*, *D. vulgaris* Miyazaki, *D. gigas* and *Desulfoarculus* (*Des.*) *baarsii*. *atf*, A-type flavoprotein; *ahp*, alkyl hydroperoxide; *bfr*, bacterioferritin; *dfx*, desulphoferrodoxin; *fr*, ferritin; *perR*, peroxidase-like repressor protein; *rbr*, rubrerythrin; *rd-2*, type 2 rubredoxin; *rd-1*, type 1 rubredoxin; *roo*, rubredoxin:oxygen-oxidoreductase; *sod*, superoxide dismutase.

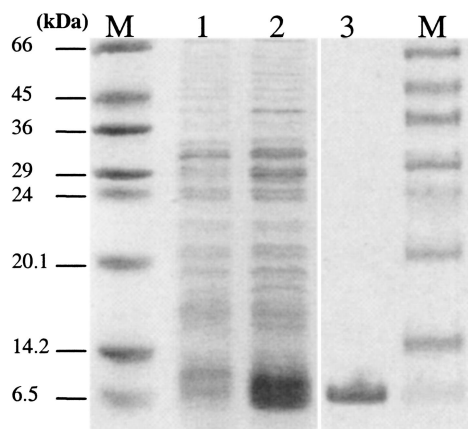


Fig. 6. Overproduction of *Dd27k* Rd-2 in aerobically grown cells of *E. coli* BL21-Gold (DE3) analysed by 15% SDS-PAGE. Lanes 1 and 2, samples of cell extracts obtained by small-scale preparations (2 ml); lane 1, *E. coli* carrying plasmid pT7-7 (control); lane 2, *E. coli* carrying plasmid pT7Rd2. Lane 3, Rd-2 as purified. The left and right margins show the positions of marker proteins (M).

well described by a sum of three exponential fluorescence lifetimes with time constants τ_i and amplitudes α_i , as presented in Table 1. The average fluorescence lifetime of ZnRd-2 alone is 1.26 ns (obtained with eqn 1; see *Experimental procedures*). After the addition of Bfr, the fluorescence decay of Rd-2 is still described by the sum of three exponentials, but the average excited state lifetime, $\langle \tau \rangle$, increases to 2.25 ns and 2.32 ns for the mixtures Rd-2/Bfr 1:1 and 1:2 (rubredoxin per Bfr monomer). The three components obtained in the presence of Bfr differ from those of Rd-2 alone (Table 1), and there is no evidence of a specific interaction with a given chromophore. The increase in the average fluorescence lifetime as a result of the presence of Bfr can only be attributed to a change in the microenvironment of the Trp(s) from Rd-2, indicating that there is a direct interaction between the two proteins in solution.

Further evidence for the Rd-2–Bfr association is obtained from comparison of the steady-state anisotropy of the fluorescence emission of Rd-2 at 350 nm, when excited at 300 nm, in the presence and absence of Bfr (Table 1). With the addition of Bfr, an increase in the steady-state fluorescence anisotropy, r , is observed, indicating a smaller diffusional rotation of the tryptophan(s) of Rd-2 before emission. This increase in steady-state fluorescence anisotropy is concomitant with an increase in the average fluorescence lifetime. Therefore, it may be concluded that there is a true hindrance to the rotation of the tryptophan(s) as a result of the larger hydrodynamic volume of the whole tumbling complex or a lower freedom of the tryptophan(s) rotation, or both. This decrease in correlation time for the rotation must result from the formation of a Rd-2–Bfr aggregate living for at least a time comparable with that of the chromophore. A comparison of the variation of fluorescence lifetime and anisotropy upon

increasing the Bfr concentration (from 1:1 and 1:2) shows that, when doubling the concentration of Bfr, only a very small increase in both is observed. This allows us to conclude that the association between the two proteins is stable and almost complete when the two proteins are mixed in a 1:1 ratio.

The reduction potential of Rd-2 (+25 mV (LeGall *et al.*, 1998)) is suitable for direct electron donation to Bfr, as the reduction potential of the haem centre was determined to be +140 mV (Romão *et al.*, 2000a), and the reduction potentials of the di-iron sites are usually quite positive (e.g. Wang *et al.*, 1991). Therefore, the redox interaction was studied by adding FeRd-2, previously reduced with dithionite (using slightly substoichiometric amounts of dithionite), to an anaerobic sample of bacterioferritin (Fig. 8, curves a to e). Under these conditions, Rd-2 reduces Bfr, and complete reduction was observed after the addition of ≈ 2.5 -fold excess per Bfr monomer. No further reduction was observed with the addition of sodium dithionite (Fig. 8, curve f), confirming that Bfr was totally reduced. This result fully agrees with the fact that *Dd27k* Bfr is isolated containing an oxidized di-iron centre per subunit and one haem per dimer (Romão *et al.*, 2000a; Coelho *et al.*, 2001). Thus, it is shown that Rd-2 donates electrons to *Dd27k* Bfr. This role may be quite relevant as the release of iron from ferritin occurs only upon reduction of the iron core (Harrison and Arosio, 1996; Theil *et al.*, 2000). These data also suggest that the electrons are donated through the haem, as an almost complete reduction of the haem is observed first (Fig. 8, curve c),

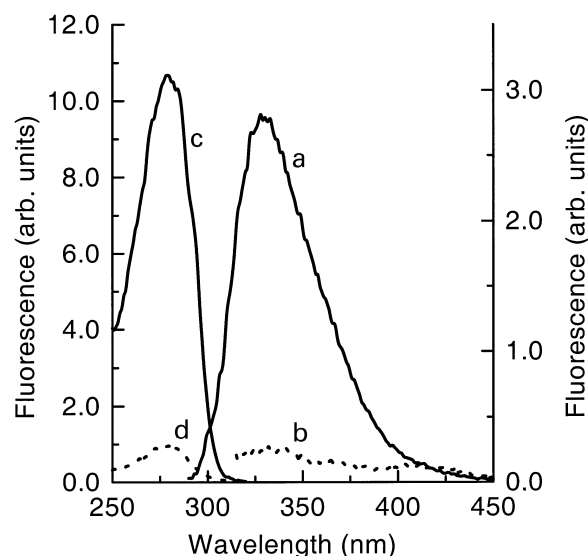


Fig. 7. Fluorescence excitation and emission spectra of 6 μ M ZnRd-2 (solid lines) and 6 μ M Bfr (dotted lines). a and b, emission spectra with excitation at 300 nm; c and d, excitation spectra with fluorescence collected at 350 nm. The fluorescence intensity units are the same for all spectra, but curves a and b are represented on an expanded scale (right axis).

Table 1. Results from the analysis of the fluorescence decay of ZnRd-2 at 350 nm, excited at 292 nm, with a sum of three exponentials with amplitudes α_i and time constants τ_i .

	Rd	Rd/Bfr 1:1	Rd/Bfr 1:2
α_1 (a.u.)	0.178	0.168	0.145
τ_1 (NS)	0.61	0.60	0.48
α_2 (a.u.)	0.154	0.165	0.215
τ_2 (NS)	1.37	1.30	1.21
α_3 (a.u.)	0.0026	0.030	0.033
τ_3 (NS)	4.98	4.78	4.90
$\langle \tau \rangle$ (NS)	1.26	2.25	2.32
r	0.12 ₃	0.13 ₄	0.13 ₇

The average lifetime, $\langle \tau \rangle$, is calculated using eqn 1. The values of the steady-state fluorescence anisotropy, r , obtained with excitation at 300 nm and observation at 350 nm are also presented. Mixture 1:1, one rubredoxin per one monomer of Bfr; mixture 1:2, one rubredoxin per two monomers of Bfr. Protein concentration, ZnRd-2 = 6 μ M; Bfr = 6 μ M (mixture 1:1) and 12 μ M (mixture 1:2).

but reoxidation of Rd-2 continues to occur, presumably because the di-iron centres are being reduced (Fig. 8, curve d).

In *E. coli*, the bacterioferritin-associated ferredoxin, Bfd, was shown to form a complex *in vitro* with Bfr (Garg *et al.*, 1996), a behaviour similar to that now shown to occur for Dd27k Bfr and Rd-2. It remains to be demonstrated that Bfd is also an electron donor for Bfr, although this function has already been proposed (Garg *et al.*, 1996). If this proves to be true, Rd-2 and Bfd would play similar roles in iron metabolism.

Conclusion

In the sulphate-reducing bacterium *D. desulphuricans* ATCC 27774, the genes encoding for bacterioferritin and rubredoxin-2 are under the same transcription regulation, forming a dicistronic operon. This genetic arrangement, so far unique among bacteria, together with the evidence for the formation of a complex and the electron transfer between Bfr and Rd-2 strongly suggests a physiological relationship between the two proteins. In addition, it makes rubredoxin-2 the only known example of a redox partner for an iron storage protein, paralleling the proposed function for Bfd in other systems (Garg *et al.*, 1996). This finding also enlarges the known physiological functions of rubredoxins in anaerobes, particularly in *Desulfovibrio* species. Both genetic and biochemical data indicate that, in these bacteria, rubredoxins are involved in both oxygen and iron metabolisms.

Experimental procedures

Cloning and sequencing of rubredoxin and bacterioferritin genes

Genomic DNA from Dd27k was grown, isolated and purified

as described previously (Liu and Peck, 1981; Ausubel *et al.*, 1995).

Standard protocols (Ausubel *et al.*, 1995) were used for DNA manipulation. Restriction enzymes and the digoxigenin (DIG) non-radioactive nucleic acid labelling and detection system were obtained from Roche Molecular Biochemicals. Purification of plasmids, polymerase chain reaction (PCR) products and DNA fragments from gel agarose was achieved with Concert DNA purification systems from Gibco BRL Life Technologies.

Based on the N-terminal amino acid sequences of Dd27k Rd-2 (LeGall *et al.*, 1998) and Bfr (Romão *et al.*, 2000a) and on the *Desulfovibrio* codon usage (Stokkermans *et al.*, 1992), a pair of degenerate oligonucleotides was designed for each protein (Table 1). Internal segments of 117 bp for *rd-2* and 196 bp for *bfr* were amplified by PCR with *Taq* polymerase, using Dd27k genomic DNA as template and the corresponding pair of oligonucleotides. For sequencing purposes, the two PCR products were cloned. To this end, the rubredoxin DNA fragment was purified, end repaired with Klenow polymerase and cloned in *EcoRV* digested/desphosphorylated pBlue-script SK+, yielding pSRd1. The transformation was performed in *E. coli* DH5 α cells. Bacterioferritin PCR product was also purified, end repaired, ligated to *EcoRV*-cut pZErOTM-1 (Invitrogen), yielding pZBfr1, and the mixture was transformed in *E. coli* XL2-Blue cells (Promega). Recombinant plasmids, pSRd1 and pZBfr1, were isolated, sequenced with the ABI Prism BigDye terminator cycle sequencing ready reaction kit (PE Biosystems) and analysed on an Applied Biosystems 377A DNA sequencer. The results confirmed that the desired DNA fragments were cloned. After excision of the inserts from plasmids pSRd1 and pZBfr1, two homologous DIG-labelled DNA probes were then prepared using the random primed DNA labelling system.

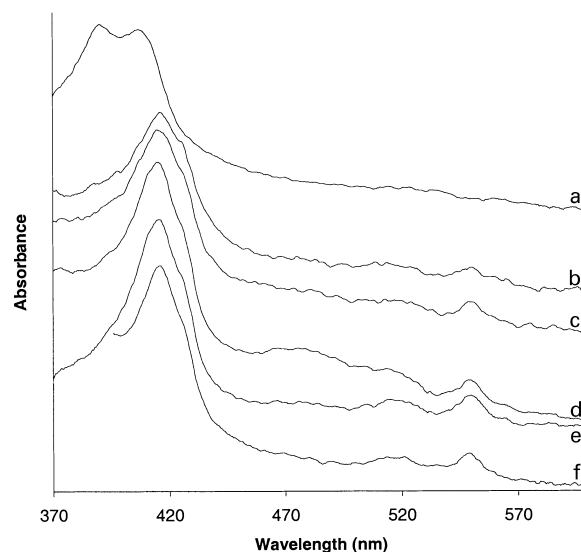


Fig. 8. Visible spectra after the reduction of Bfr after adding FeRd-2 under anaerobic conditions in 20 mM phosphate buffer, pH 7.6. (a) Bfr; (b) after the addition of FeRd-2 previously reduced with dithionite; (c) the same as (b) but after 5 min; (d) after 20 min (some FeRd-2 reoxidized is observed); (e) the same as (d) subtracting the spectrum of oxidized FeRd-2; (f) after reduction with dithionite. Protein concentrations, Bfr = 3 μ M (monomer); FeRd-2 = 7.5 μ M.

Southern blots of *Dd27k* genomic DNA digested with several restriction enzymes were hybridized with the DIG-labelled *bfr* and the DIG-labelled *rd-2*. The *rd-2* probe was also used to screen a previously constructed λ -Dash genomic library of *Dd27k* (Lambda Dash II/*Bam*HI vector kit and Gigapack III gold packaging extract from Stratagene). The library was used to infect *E. coli* XL1 Blue MRA-P2 cells, and the phages containing the rubredoxin gene were identified by plaque hybridization with the DIG-labelled *rd-2* probe, according to the DIG system protocols. Two positive phages (named phages 6 and 11) were then purified, and phage DNA was isolated with the Lambda maxi kit from Qiagen.

The restriction maps retrieved from the Southern blots of digested *Dd27k* genomic DNA and DNA isolated from phage 6 indicated that the rubredoxin and bacterioferritin genes were located in the same 3 kb *Eco*RI–*Sph*I fragment (Fig. 1). Southern blots of the second phage (phage 11) showed that both genes (*bfr* and *rd-2*) were contained in a 2.5 kb *Eco*RI–*Sph*I fragment (where *Eco*RI is the restriction site of the arm phage). Hence, that insert was cleaved from phage 11 DNA, ligated into *Eco*RI–*Sph*I-cut pUC18, and the mixture was used to transform *E. coli* JM109 cells (Promega). Recombinant plasmids, named pUBfRd, were isolated and sequenced on both strands. The results showed that this clone contained another ORF coding for a protein with significant similarity to the peroxidase-like repressor family of proteins (PerR). However, the 2.5 kb *Eco*RI–*Sph*I fragment of plasmid pUBfRd contained only part of the *perR*-like gene. In order to assess the complete *perR*-like gene sequence, direct sequencing of phage 6 DNA was performed.

The sequences were deposited in the GenBank sequence database under the accession number AF321851.

The nucleotide sequence data were analysed using MULTIPLE sequence alignment with hierarchical clustering (Corpet *et al.*, 1988), the Genetics Computer Group (Wisconsin) package provided by the Portuguese EMBnet Node (PEN) and Neural Networks for Promoter Prediction (Reese *et al.*, 1996). The BLAST network service at NCBI and the CLUSTAL X program (Thompson *et al.*, 1994) allowed the production amino acid sequence alignments.

Preliminary sequence data of the *D. vulgaris* Hildenborough genome was obtained from The Institute for Genomic Research website at <http://www.tigr.org>.

Overexpression, isolation and purification of the recombinant *Dd27k Rd-2*

For expression purposes, homologous oligonucleotides were designed that allowed the introduction in the *rd-2* gene of an *Eco*RI restriction site at the start codon and a *Hind*III restriction site downstream of the stop codon (Table 2). By means of a PCR reaction, using the oligonucleotides, *Pfu* polymerase (Stratagene) and pUBfRd plasmid, amplification of the complete *rd-2* gene (218 bp) was then achieved. After purification, the 218 bp fragment of *rd-2* was cloned in pT7-7 (Ausubel *et al.*, 1995), previously cut with the appropriate restriction enzymes, and transformed in *E. coli* DH5 α cells. The resultant recombinant plasmid, pT7Rd2, was isolated and sequenced to ensure the integrity of the gene. Cultures of BL21-Gold (DE3) (Stratagene) containing pT7Rd2 were

grown, aerobically and at 37°C, in a 3l fermenter in M9 minimal medium (Ausubel *et al.*, 1995) containing 100 μ g of ampicillin and were induced with 400 μ M IPTG when an OD₆₀₀ of 0.8 was reached. The cells were harvested after 4 h and resuspended into 10 mM Tris-HCl, pH 7.6, broken in a French pressure cell (SLM; Aminco) at 9000 psi. By ultracentrifugation (150 000 g, 1 h), the membranes and cell debris were removed, and the soluble extract obtained was submitted to further purification.

All purification procedures were performed at 4°C in a Pharmacia High-Load System, and proteins were concentrated using a Diaflo apparatus (Amicon) with a YM3 membrane. The prepared soluble extract was loaded on a Q-Sepharose XK26/14 column, previously equilibrated with 20 mM Tris-HCl, pH 7.6. A gradient up to 0.5 M NaCl, in the same buffer (3 ml min⁻¹), was then applied, and the Rd-2 fraction was eluted at 0% NaCl. This fraction was purified further by gel filtration on a Superdex 75 (XK26/50) column using 20 mM Tris-HCl, pH 7.6, 0.2 M NaCl (0.75 ml min⁻¹) as elution buffer. The fraction containing Rd-2 was then dialysed against 20 mM Tris-HCl, pH 7.2, over 24 h and applied to a SP-Sepharose column (XK 16/12), previously equilibrated with 20 mM Tris-HCl, pH 7.2. A gradient of 0–0.5 M NaCl (1 ml min⁻¹) in the same buffer was used. The two rubredoxin forms usually observed, the zinc and iron forms, could be separated completely under these conditions. The major form, the iron-Rd-2, represents 60% of the total amount of produced Rd-2 and was eluted with 0.25 M NaCl, whereas the zinc-Rd-2 form was eluted at 0.05 M NaCl. The zinc and iron forms will be designated as ZnRd-2 and FeRd-2 respectively. The purity of Rd-2 was judged by 15% SDS-PAGE and by UV-visible spectroscopy (absorbance ratio A₂₈₀/A₄₈₀ = 2.71 for FeRd-2). Metal analysis was performed by Atomic Absorption at Laboratório de Análises, IST-Lisbon, and protein concentration was determined by bicinchoninic acid (BCA) protein assay kit (Pierce) as described by Smith *et al.* (1985).

Bacterioferritin was purified as described previously (Romão *et al.*, 2000a).

RNA isolation and Northern analyses

RNA was extracted from *Dd27k* cells grown anaerobically with nitrate and collected at the initial, mid-log and late-exponential phases and from *Dd27k* cells grown anaerobically with sulphate and collected at the initial exponential phase. Total RNA was isolated with the Qiagen RNeasy extraction kit and finally resuspended in diethyl pyrocarbonate (DEPC)-treated

Table 2. Synthetic oligonucleotides used to amplify, by PCR, the different internal segments of the *rd-2* and *bfr* genes that were used as DNA or RNA probes and for expression purposes.

<i>rd-2</i>	DNA probe	5'-GCSGARCCSCAGGAYATG-3' 5'-SGGVAGRTCCTCGAAGCTTSG-3'
	Expression	5'-GCTGAATTCCTACCGGAAAAACAATAGG-3'
	RNA probe	5'-CCGGTACGCATGAAGCTTCTTATG-3'
<i>bfr</i>	DNA probe	5'-MGNAAGGCVAAGGTVATMGARGTVC-3' 5'-CVCCVCCVAGYTCTTKATNCKYTC-3'
	RNA probe	5'-CACAAAGGAGTTTCCATATGGCTGG-3' 5'-GTTTTCCGGAAGCTTTTCAGCAGC-3'

water. Samples of 0.5–1 µg of total RNA were electrophoresed on 1.2% (w/v) agarose (Seakem LE; FMC) gels in 1× FA buffer (10× formaldehyde buffer: 200 mM MOPS, 50 mM sodium acetate and 10 mM EDTA, pH 7) containing 0.7% (v/v) formaldehyde and transferred to positively charged nylon membranes (Roche Molecular Biochemicals).

Two homologous oligonucleotides (Table 2) were used in a PCR reaction together with plasmid pUBfRd and *Pfu* polymerase (Stratagene) to amplify the *bfr* gene (568 nt). The fragment was then cloned in pZErOTM-1 previously cut with *EcoRV*, yielding plasmid pZBfr2. Also, the 218 bp *rd-2* PCR product prepared for overexpression purposes, as described above, was cloned in *EcoRV*-digested pZErOTM-1 and named pZRd3. In both cases, *E. coli* XL2-Blue cells were used for transformation. After isolation, the recombinant plasmids were linearized with *EcoRI* and used as templates to generate two antisense RNA probes, according to the DIG RNA labelling kit (SP6/T7) (Roche Molecular Biochemicals). Northern blots of *Dd27k* RNA were then hybridized with the prepared *rd-2* and *bfr* RNA probes.

Steady-state and time-resolved fluorescence spectroscopy

Samples were obtained at the appropriate concentrations by diluting the protein stock solutions into a 20 mM phosphate buffer, pH 7.6. The zinc form of Rd-2 was used, and all the assays were performed at room temperature. Steady-state fluorescence spectra and single-wavelength fluorescence anisotropy were obtained with an SLM-Aminco 8100-2 spectrofluorometer. The values of fluorescence anisotropy result from the average of at least 10 independent measurements. Fluorescence decays are measured by the single photon counting technique using a Ti:Sapphire picosecond laser system (Spectra Physics) operating at a repetition rate of 827 kHz, and the excitation wavelength was tuned to 292 nm. The pulse profile and the emission of the sample at 350 nm were collected in alternate cycles of 10³ counts each until a total accumulation of 5 × 10³ counts at the maximum. Deconvolution of the fluorescence decay from the pulse profile was carried out using a version of George Striker's program (Striker, 1982). Average lifetimes, $\langle \tau \rangle$, were calculated with eqn 1, where α_i stands for the relative weight of the component with lifetime τ_i .

$$\langle \tau \rangle = \frac{\sum_i \alpha_i \tau_i^2}{\sum_i \alpha_i \tau_i} \quad (1)$$

Acknowledgements

We thank Professor António Maçanita (ITQB) for the time-resolved fluorescence spectroscopy studies. The work was supported by FCT grant 36558/99 to MT. P.N.C. and C.V.R. acknowledge Praxis XXI grants BD/9167/96 and BD/19879/99.

References

Andrews, S.C. (1998) Iron storage in bacteria. *Adv Microb Physiol* **40**: 281–349.

Ascenso, C., Rusnak, F., Cabrito, I., Lima, M.J., Naylor, S.,

Moura, I., and Moura, J.J. (2000) Desulfoferrodoxin: a modular protein. *J Biol Inorg Chem* **5**: 720–729.

Ausubel, F.M., Brent, R., Kingston, R.E., Moore, D.D., Seidman, J.G., Smith, J.A., and Struhl, K. (1995) *Current Protocols in Molecular Biology*. New York: Greene Publishing Associates and Wiley Interscience.

Brumlik, M.J., and Voordouw, G. (1989) Analysis of the transcriptional unit encoding the genes for rubredoxin (*rub*) and a putative rubredoxin oxidoreductase (*rbo*) in *Desulfovibrio vulgaris* Hildenborough. *J Bacteriol* **171**: 4996–5004.

Bruschi, M., Moura, I., LeGall, J., Xavier, A.V., Sieker, L.C., and Couchoud, P. (1979) The amino acid sequence of desulfoferrodoxin, a new type of non heme iron protein from *Desulfovibrio gigas*. *Biochem Biophys Res Commun* **90**: 596–605.

Bsat, N., Herbig, A., Casillas-Martinez, L., Setlow, P., and Helmann, J.D. (1998) *Bacillus subtilis* contains multiple Fur homologues: identification of the iron uptake (Fur) and peroxide regulon (PerR) repressors. *Mol Microbiol* **29**: 189–198.

Bulen, W.A., LeComte, J.R., and Lough, S. (1973) A hemoprotein from *Azotobacter* containing non-heme iron: isolation and crystallization. *Biochem Biophys Res Commun* **54**: 1274–1281.

Bult, C.J., White, O., Olsen, G.J., Zhou, L., Fleischmann, R.D., Sutton, G.G., et al. (1996) Complete genome sequence of the methanogenic archaeon, *Methanococcus jannaschii*. *Science* **273**: 1058–1073.

Chen, C.-Y., and Morse, S.A. (1999) *Neisseria gonorrhoeae* bacterioferritin: structural heterogeneity, involvement in iron storage and protection against oxidative stress. *Microbiology* **145**: 2967–2975.

Chen, L., Liu, M.Y., LeGall, J., Fareleira, P., Santos, H., and Xavier, A.V. (1993) Rubredoxin oxidase, a new flavo-hemoprotein, is the site of oxygen reduction to water by the 'strict anaerobe' *Desulfovibrio gigas*. *Biochem Biophys Res Commun* **193**: 100–105.

Coelho, A.V., Macedo, S., Matias, P.M., Thompson, A.W., LeGall, J., and Carrondo, M.A. (2001) Structure determination of bacterioferritin from *Desulfovibrio desulfuricans* by the MAD method at the Fe K-edge. *Acta Crystallogr* **D57**: 326–329.

Corpet, F. (1988) Multiple sequence alignment with hierarchical clustering. *Nucleic Acids Res* **16**: 10881–10890.

Eidsness, M.K., Burden, A.E., Richie, K.A., Kurtz, D.M., Jr, Scott, R.A., et al. (1999) Modulation of the redox potential of the [Fe(SCys)₄] site in rubredoxin by the orientation of a peptide dipole. *Biochemistry* **38**: 14803–14809.

Frazão, C., Silva, G., Gomes, C.M., Matias, P., Coelho, R., Sieker, L., et al. (2000) Structure of a dioxygen reduction enzyme from *Desulfovibrio gigas*. *Nature Struct Biol* **7**: 1041–1045.

Frolow, F., Kalb, A.J., and Yariv, J. (1994) Structure of a unique twofold symmetric haem-binding site. *Nature Struct Biol* **1**: 453–460.

Garg, R.P., Vargo, C.J., Cui, X., and Kurtz, D.M. (1996) A [2Fe-2S] protein encoded by an open reading frame upstream of the *Escherichia coli* bacterioferritin gene. *Biochemistry* **35**: 6297–6301.

Gomes, C.M., Silva, G., Oliveira, S., LeGall, J., Liu, M.Y., Xavier, A.V., et al. (1997) Studies on the redox centers of

- the terminal oxidase from *Desulfovibrio gigas* and evidence for its interaction with rubredoxin. *J Biol Chem* **272**: 22502–22508.
- Gomes, C.M., Vicente, J.B., Wasserfallen, A., and Teixeira, M. (2000) Spectroscopic studies and characterization of a novel electron-transfer chain from *Escherichia coli* involving a flavorubredoxin and its flavoprotein reductase partner. *Biochemistry* **39**: 16230–16237.
- Harrison, P.M., and Arosio, P. (1996) The ferritins: molecular properties, iron storage function and cellular regulation. *Biochim Biophys Acta* **1275**: 161–203.
- Kitamura, M., Koshino, Y., Kamikawa, Y., Kohno, K., Kojima, S., Miura, K., et al. (1997) Cloning and expression of the rubredoxin gene from *Desulfovibrio vulgaris* (Miyazaki F) – comparison of the primary structure of desulfoferrodoxin. *Biochim Biophys Acta* **1351**: 239–247.
- Kummerle, R., Zhuang-Jackson, H., Gaillard, J., and Moulis, J.M. (1997) Site-directed mutagenesis of rubredoxin reveals the molecular basis of its electron transfer properties. *Biochemistry* **36**: 15983–15991.
- LeGall, J., Pickril, B.C., Moura, I., Xavier, A.V., Moura, J.J., and Huynh, B.H. (1988) Isolation and characterization of rubrerythrin, a non-heme iron protein from *Desulfovibrio vulgaris* that contains rubredoxin centers and a hemerythrin-like binuclear iron cluster. *Biochemistry* **27**: 1636–1642.
- LeGall, J., Liu, M.Y., Gomes, C.M., Braga, V., Pacheco, I., Regalla, M., et al. (1998) Characterisation of a new rubredoxin isolated from *Desulfovibrio desulfuricans* 27774: definition of a new family of rubredoxins. *FEBS Lett* **429**: 295–298.
- Liochev, S.I., and Fridovich, I. (1997) A mechanism for complementation of the sodA sodB defect in *Escherichia coli* by overproduction of the *rbo* gene product (desulfoferrodoxin) from *Desulfoarculus baarsii*. *J Biol Chem* **272**: 25573–25575.
- Liu, M.C., and Peck, H.D. (1981) The isolation of a hexaheme cytochrome from *Desulfovibrio desulfuricans* and its identification as a new type of nitrite reductase. *J Biol Chem* **256**: 13159–13164.
- Lumppio, H.L., Shenvi, N.V., Garg, R.P., Summers, A.O., and Kurtz, D.M., Jr (1997) A rubrerythrin operon and nigerythrin gene in *Desulfovibrio vulgaris* (Hildenborough). *J Bacteriol* **179**: 4607–4615.
- Moulis, J.M. (1999) Information about the biologically relevant properties of *Clostridium pasteurianum* rubredoxin obtained from modelling and dynamics simulations of molecular variants. *Theor Chem Acc* **101**: 223–227.
- Pianzola, M.J., Soubes, M., and Touati, D. (1996) Overproduction of the *rbo* gene product from *Desulfovibrio* species suppresses all deleterious effects of lack of superoxide dismutase in *Escherichia coli*. *J Bacteriol* **178**: 6736–6742.
- Ragsdale, S.W., Ljungdahl, L.G., and DerVartanian, D.V. (1983) Isolation of carbon monoxide dehydrogenase from *Acetobacterium woodii* and comparison of its properties with those of the *Clostridium thermoaceticum* enzyme. *J Bacteriol* **155**: 1224–1237.
- Ratnayake, D.B., Wai, S.N., Shi, Y., Amako, K., Nakayama, H., and Nakayama, K. (2000) Ferritin from the obligate anaerobe *Porphyromonas gingivalis*: purification, gene cloning and mutant studies. *Microbiology* **146**: 1119–1127.
- Reese, M.G., Harris, N.L., and Eeckman, F.H. (1996) Large Scale Sequencing Specific Neural Networks for Promoter and Splice Site Recognition. In *Biocomputing: Proceedings of the 1996 Pacific Symposium*. Hunter, L., and Klein, T.E. (eds). Singapore: World Scientific Publishing, pp. 737–738.
- Rocha, E.R., Andrews, S.C., Keen, J.N., and Brock, J.H. (1992) Isolation of a ferritin from *Bacteroides fragilis*. *FEMS Microbiol Lett* **74**: 207–212.
- Romão, C.V., Liu, M.Y., LeGall, J., Gomes, C.M., Braga, V., Pacheco, I., et al. (1999) The superoxide dismutase activity of desulfoferrodoxin from *Desulfovibrio desulfuricans* ATCC 27774. *Eur J Biochem* **261**: 438–443.
- Romão, C.V., Regalla, M., Xavier, A.V., Teixeira, M., Liu, M.Y., and LeGall, J. (2000a) A bacterioferritin from the strict anaerobe *Desulfovibrio desulfuricans* ATCC 27774. *Biochemistry* **39**: 6841–6849.
- Romão, C.V., Louro, R., Timkovich, R., Lubben, M., Liu, M.Y., LeGall, J., et al. (2000b) Iron-coproporphyrin III is a natural cofactor in bacterioferritin from the anaerobic bacterium *Desulfovibrio desulfuricans*. *FEBS Lett* **480**: 213–216.
- Sieker, L.C., Stenkamp, R.E., and LeGall, J. (1994) Rubredoxin in crystalline state. *Methods Enzymol* **243**: 203–216.
- Smith, D.R., Doucette-Stamm, L.A., Deloughery, C., Lee, H., Dubois, J., Aldredge, T., et al. (1997) Complete genome sequence of *Methanobacterium thermoautotrophicum* deltaH: functional analysis and comparative genomics. *J Bacteriol* **179**: 7135–7155.
- Smith, P.K., Krohn, R.I., Hermanson, G.T., Mallia, A.K., Gartner, F.H., Provenzano, M.D., et al. (1985) Measurement of protein using bicinchoninic acid. *Anal Biochem* **150**: 76–85.
- Stiefel, E.I., and Watt, G.D. (1979) *Azotobacter* cytochrome *b*_{557.5} is a bacterioferritin. *Nature* **279**: 81–83.
- Stokkermans, J.P., Pierik, A.J., Wolbert, R.B., Hagen, W.R., Van Dongen, W.M., and Veeger, C. (1992) The primary structure of a protein containing a putative [6Fe-6S] prismatic cluster from *Desulfovibrio vulgaris* (Hildenborough). *Eur J Biochem* **208**: 435–442.
- Striker, G. (1982) Effective implementation of modulation function. In *Deconvolution and Reconvolution of Analytical Signals*. Bouchy, M. (ed.). Nancy: DPIC, pp. 329–354.
- Swartz, P.D., Beck, B.W., and Ichiye, T. (1996) Structural origins of redox potentials in Fe-S proteins: electrostatic potentials of crystal structures. *Biophys J* **71**: 2958–2969.
- Tabata, S., Kaneko, T., Nakamura, Y., Kotani, H., Kato, T., Asamizu, E., et al. (2000) Sequence and analysis of chromosome 5 of the plant *Arabidopsis thaliana*. *Nature* **408**: 823–826.
- Theil, E.C. (1987) Ferritin: structure, gene regulation, and cellular function in animals, plants, and microorganisms. *Annu Rev Biochem* **56**: 289–315.
- Theil, E.C., Takagi, H., Small, G.W., He, L., Tipton, A.R., and Danger, D. (2000) The ferritin iron entry and exit problem. *Inorg Chim Acta* **297**: 242–251.
- Thompson, J.D., Higgins, D.G., and Gibson, T.J. (1994) CLUSTAL W: improving the sensitivity of progressive multiple sequence alignment through sequence weighting, position-specific gap penalties and weight matrix choice. *Nucleic Acids Res* **22**: 4673–4680.
- Waldo, G.S., and Theil, E.C. (1996) Ferritin and Iron

- Biomineralization. In *Comprehensive Supramolecular Chemistry*, Vol. 5. Supramolecular Reactivity and Transport: Bioinorganics Systems. Suslick, K.S. (ed.). Oxford: Pergamon, pp. 65–89.
- Wang, D.L., Holz, R.C., David, S.S., Que, L., and Stankovich, M.T. (1991) Electrochemical properties of the diiron core of uteroferrin and its anion complexes. *Biochemistry* **30**: 8187–8194.
- Wastl, J., Sticht, H., Maier, U.G., Rosch, P., and Hoffmann, S. (2000) Identification and characterization of a eukaryotically encoded rubredoxin in a cryptomonad alga. *FEBS Lett* **471**: 191–196.
- Yariv, J., Kalb, A.J., Sperling, R., Bauminger, E.R., Cohen, S.G., and Ofer, S. (1981) The composition and the structure of bacterioferritin of *Escherichia coli*. *Biochem J* **197**: 171–175.
- Yoon, K.S., Hille, R., Hemann, C., and Tabita, F.R. (1999) Rubredoxin from the green sulfur bacterium *Chlorobium tepidum* functions as an electron acceptor for pyruvate ferredoxin oxidoreductase. *J Biol Chem* **274**: 29772–29778.
- Zauner, S., Fraunholz, M., Wastl, J., Penny, S., Beaton, M., Cavalier-Smith, T., *et al.* (2000) Chloroplast protein and centrosomal genes, a tRNA intron, and odd telomeres in an unusually compact eukaryotic genome, the cryptomonad nucleomorph. *Proc Natl Acad Sci USA* **97**: 200–205.